Molecular Biology of the Cell
Vol. 9, 1609–1612, July 1998

Video Essay

Imaging of Echinoderm Fertilization[1]V

Mark Terasaki

Department of Physiology, University of Connecticut Health Center, Farmington, Connecticut 06032

Monitoring Editors: Jennifer Lippincott-Schwartz and W. James Nelson

INTRODUCTION

Eggs from echinoderms (sea urchin, starfish, and sand dollars) have been an excellent subject for cell biology for more than 100 years. Among the many discoveries that have been made with echinoderm eggs are the first studies of the centrosome (Boveri, 1902; also see Baltzer, 1967), the Ca requirement for healing plasma membrane wounds (Chambers, 1917) with the subsequent hypothesis of a central role of Ca in cell physiology (summarized by Heilbrunn, 1958), relationships of the mitotic apparatus and cytokinetic furrow (Rappaport, 1986), and the first identification of cyclins (Evans *et al.*, 1983).

Why have echinoderm eggs been so productive experimentally? There are probably several reasons. Marine eggs are autonomous and develop normally in sea water, an easily reproduced environment. Echinoderm fertilization is reliable and sets into motion many fundamental cell biological processes. The eggs are relatively clear, so that changes in organization deep in the cytoplasm can be viewed by light microscopy. For biochemical studies, the eggs can be obtained as a homogeneous population in large quantities.

With the resurgence of light microscopy in the last 20 years or so, new tools, techniques, and reagents have become available to make new discoveries and to see more clearly what was known or previously only deduced. These movies show several views of fertilization of sea urchin (*Lytechinus variegatus* and *Lytechinus pictus*) and starfish (*Asterina miniata*) eggs.

VIDEO SEQUENCES

Sequence 1 (Figure 1) shows simultaneous double imaging of phase contrast (left) and intracellular Ca concentration (right) during sea urchin egg fertilization. The transmitted light image shows the approach of the sperm at about 2 o'clock and the rising of the fertilization envelope. Intracellular Ca is monitored by Ca green dextran (20 μM), an indicator that becomes more fluorescent when it binds Ca. A transient Ca rise around the entire cortex (fifth frame) is followed by the Ca wave, which begins at the sperm entry site. The rapid cortical rise is due to Ca entry through voltage-gated channels; this Ca action potential constitutes the fast block to polyspermy (Jaffe, 1976). A wave of Ca release from the endoplasmic reticulum (ER) at fertilization occurs in many organisms (Gilkey *et al.*, 1978). In sea urchin eggs, it triggers exocytosis of cortical granules, which leads to elevation of the fertilization envelope. The interval between the first nine frames is 0.5 s, and it is 1.5 s for the following frames. The egg is ~105 μm in diameter.

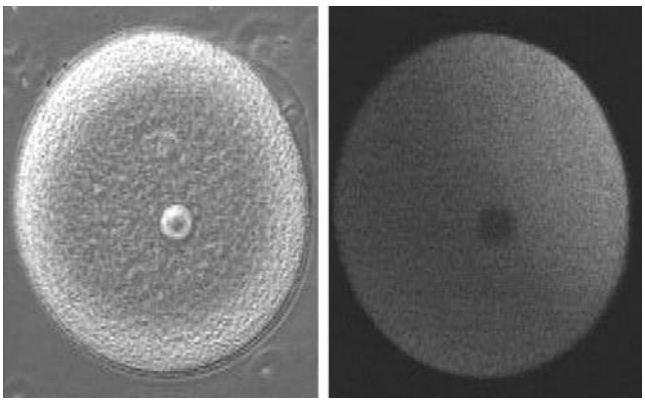

Figure 1. Double imaging of phase contrast and intracellular Ca concentration during fertilization.

Sequence 2 (Figure 2) shows simultaneous double imaging showing intracellular Ca and the approach of the sperm (starfish). Egg extracellular components trigger the sperm to undergo the acrosome reaction; the acrosomal vesicle inside the sperm fuses with the sperm plasma membrane, and actin polymerization pushes out this new region of plasma membrane to form the acrosomal tubule. The thin acrosomal tubule extends from the sperm head and contacts the egg. The region of contact is of great interest, because this is where sperm-egg membrane fusion occurs and is also where signal transduction events occur that result in membrane depolarization, Ca wave initiation, and,

[1] Several of these sequences were made in collaboration with Laurinda Jaffe (University of Connecticut Health Center). Thanks also to Steve Vogel (Medical College of Georgia) for suggesting the use of R18 to label sperm plasma membrane, and Tom Reese (National Institute of Neurological Diseases and Stroke, National Institutes of Health) in whose lab many of these sequences were obtained.

V Online version contains video information for Figures 1–6. Online version available at www.molbiolcell.org.

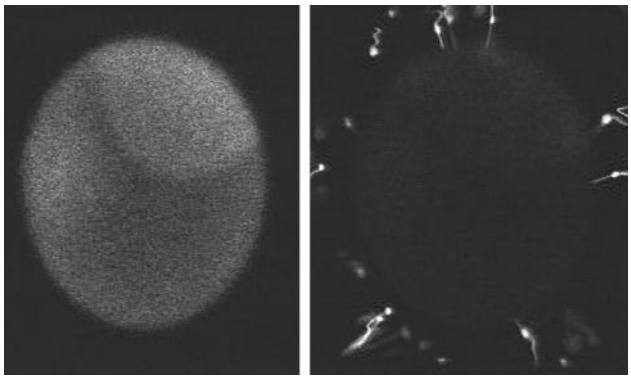

Figure 2. Intracellular Ca and the approach of the sperm.

later on, actin polymerization. The starfish acrosomal tubule is particularly long, ~10 μm. The left panel of the movie shows Ca green dextran fluorescence (20 μM), and the right panel shows sperm whose plasma membraneshavebeenlabeledwithR18(octadecylrhodamine). It is not possible to tell whether the fertilizing sperm is the one seen in the sequence near the top or is another sperm out of the focal plane. R18 was dissolved at 10 mM in ethanol and diluted 1:1000 to label the sperm. The interval between images is 1 s. The egg is ~180 μm in diameter.

Sequence 3 (Figure 3) shows simultaneous double imaging of cortical granule exocytosis by differential interference contrast (DIC) and a membrane stain during sea urchin egg fertilization. Cortical granules are 0.5- to 1.0-μm-diameter vesicles that line the interior of the plasma membrane. They contain enzymes that modify the preexisting vitelline layer so that it elevates to form the fertilization envelope. Freeze fracture of rapidly frozen fertilized eggs showed crater-like depressions in the plasma membrane resulting from exocytosis (Chandler and Heuser, 1979). These depressions are long lived and can be labeled with fluorescent dextrans or membrane dyes (Terasaki,

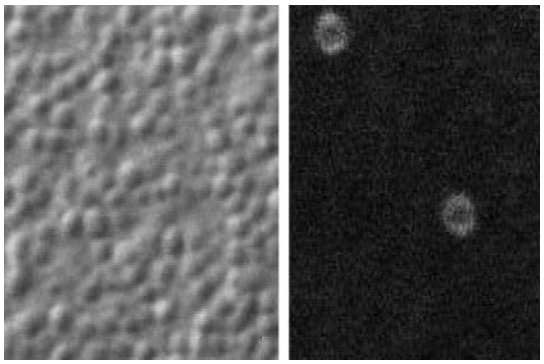

Figure 3. Cortical granule exocytosis by differential interference contrast.

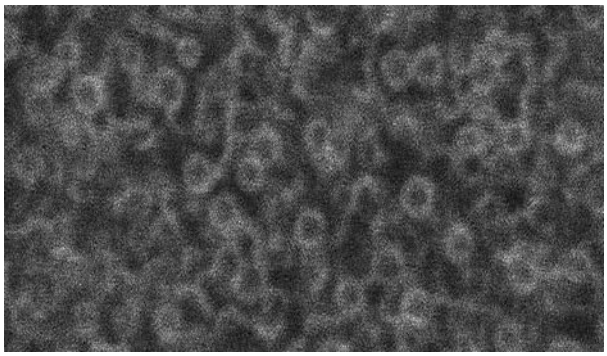

Figure 4. Structural change of ER at fertilization.

1995). Exocytosis results in hydration and release of the cortical granule contents, which eliminate the refractive index difference between the cytosol and cortical granule. Thus, by scanning DIC, which detects refractive index differences, the cortical granule "disappears" as it undergoes exocytosis (left panel of movie). The disappearance corresponds exactly to the appearance of membrane labeling of the resulting depression. The dye FM 1-43 is soluble and nonfluorescent in water and partitions into the plasma membrane where it becomes fluorescent. When FM 1-43 labels the walls of a depression, it appears in optical section as a ring (right panel). It is easiest to see the correspondence of DIC and fluorescence changes by stepping forward and backward one frame at a time within the movie. The interval between images is 0.5 s.

Sequence 4 (Figure 4) shows the structural change of ER at fertilization. The ER of starfish eggs was labeled by expression of GFP-KDEL (Terasaki *et al.*, 1996). The ER wraps around 1- to 2-μm-diameter yolk platelets so that there are many circular profiles in confocal optical sections. Fertilization results in a wave of Ca release from the ER. This movie shows the structural change in the ER that is associated with the Ca release. In the movie, the initial change in ER structure is detectable around frame 16. The structure returns to its original form by ~15 min. Photobleaching techniques showed that there is a transient disruption of ER continuity at fertilization that corresponds with the transient change in structure (Terasaki *et al.*, 1996). The interval between images is 1 s.

Sequence 5 (Figure 5) shows Rh phalloidin staining in the vicinity of the fertilization cone. After 1–2 min, the site of sperm entry develops into a cone that projects from the egg surface (the "fertilization cone"; this can be seen at the end of fert.mov of Sequence 1). This region is the site of massive actin polymerization (Tilney and Jaffe, 1980). The sea urchin egg was preinjected with 1.5 μM (final concentration) rhodamine phalloidin, a concentration that does not prevent cleavage (Terasaki, 1996). The concentration of endogenous actin is 30–70 μM. Rh phalloidin binds only to

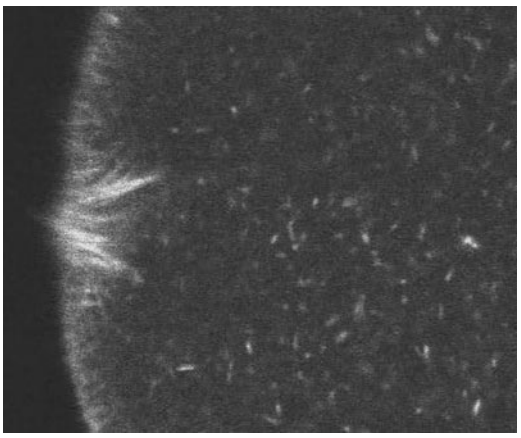

Figure 5. Rh phalloidin staining in the vicinity of the fertilization cone.

actin filaments, and when bound at a ratio of 1 phalloidin to 1 actin monomer, it stabilizes the filament against depolymerization. Its effects at lower ratios is not well characterized. Thus, it is not known to what degree this concentration of Rh phalloidin perturbs the normal actin dynamics during fertilization. Rh phalloidin staining of the fertilization cone corresponds well with images from fixed cells. However, it is uncertain whether the migration inward of actin filaments seen in the movie occurs normally. In the movie, the egg pronucleus (dark circle) enters from the right. The sperm pronucleus is barely detectable before it fuses with the egg pronucleus near the end of the sequence. Total elapsed time for this sequence is 23 min.

Sequence 6 (Figure 6) shows fusion of egg and sperm pronuclei (sea urchin). The sperm pronucleus and an associated centrosome are delivered into the egg cytoplasm by the sperm. The centrosome nucleates a microtubule aster, which enables the sperm pronucleus to move toward the center of the egg. The egg pronucleus moves on the sperm aster microtubules toward the sperm pronucleus. ER membranes also accumulate around the sperm aster. In this movie, the ER was labeled by intracellular injection of 1,1′-dioctadecyl-3,3,3′,3′-tetramethylindocarbocyanine perchlorate (DiI; Terasaki and Jaffe, 1991). The first image shows a low-magnification view of the egg with the egg pronucleus in the center (F) and a mass of ER membranes associated with the sperm pronucleus and aster (M). The movie sequence shows movement of the sperm pronucleus toward the egg pronucleus and then the fusion of the two pronuclei. The interval between frames is 10.5 s.

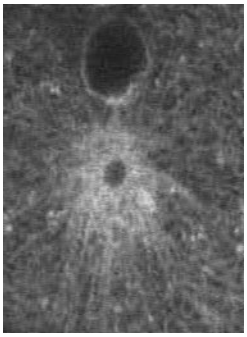

Figure 6. Fusion of egg and sperm pronuclei.

Notes on Microscopy and Movie Making

All sequences were obtained on a confocal microscope (MRC 600; Bio-Rad, Hercules, CA). When confocal microscopes first became available, the use of laser excitation led many, including myself, to conclude that photodynamic damage would prevent any studies of living cells. However, careful attention to optical conditions and instrument settings lessens photodynamic damage to the point where live-cell imaging becomes feasible. Following the lead of others (e.g., Cornell-Bell *et al.*, 1990), we found the confocal microscope to be an excellent instrument for imaging living cells. In addition to producing images with higher *z* resolution, laser scanning confocal microscopes have the advantages of built-in shuttering and digitization, as well as the convenience of "zooming" and "panning" the image. The image acquisition rate is slow compared with video, but there are many cellular processes that can be imaged usefully in time lapse.

For all of the sequences shown, images were initially recorded on an optical memory disk recorder. Images were digitized by a video capture board using Adobe Premiere (Adobe Systems, Mountain View, CA) and then made into QuickTime movies using NIH Image (National Institutes of Health, Bethesda, MD). To minimize movie size, it was necessary to reduce some images to 50–75% and to remove time points.

Macintosh users can download the program Movie Controller (1.9 MB), which allows one to vary the playback speed of QuickTime movies. More movies are available at http://www.uchc.edu/~terasaki.

REFERENCES

Baltzer, F. (1967). Theodore Boveri: Life and Work of a Great Biologist, 1862–1915, translated from German by Dorothea Rudnick, Berkeley: University of California Press.

Boveri, T. (1902). Ueber mehropolige Mitosen als Mittel zur Analyse des Zellkerns. Verh. Phys. Med. Ges. Wurzburg *35*, 67–90.

Chambers, R. (1917). Microdissection studies. I. The visible structure of cell protoplasm and death changes. Am J. Physiol. *43*, 1–12.

Chandler, D.E., and Heuser, J.E. (1979). Membrane fusion during secretion. Cortical granule exocytosis in sea urchins studied by quick-freezing and freeze fracture. J. Cell Biol. *83*, 91–108.

Cornell-Bell, A.H., Finkbeiner, S.M., Cooper, M.S., and Smith, S.J. (1990). Glutamate induces calcium waves in cultured astrocytes: long-range glial signaling. Science *247*, 470–473.

Evans, T., Rosenthal, E.T., Youngblom, J., Distel, D., and Hunt, T. (1983). Cyclin: a protein specified by maternal mRNA in sea urchin eggs that is destroyed at each cleavage division. Cell *33*, 389–396.

Gilkey, J.C., Jaffe, L.F., Ridgway, E.B., and Reynolds, G.T. (1978). A free calcium wave traverses the activating egg of the medaka, *Orizayas latipes*. J. Cell Biol. *76*, 448–466.

Heilbrunn, L.V. (1958). The Dynamics of Living Cytoplasm, New York: Academic Press.

Jaffe, L.A. (1976). Fast block to polyspermy in sea urchin eggs is electrically mediated. Nature *261*, 68–71.

Rappaport, R. (1986). Establishment of the mechanism of cytokinesis in animal cells. Int. Rev. Cytol. *105*, 245–281.

Terasaki, M. (1995). Visualization of exocytosis during sea urchin egg fertilization using confocal microscopy. J. Cell Sci. *108*, 2293–2300.

Terasaki, M. (1996). Actin filament translocations in sea urchin eggs. Cell Motil. Cytoskeleton *34*, 48–56.

Terasaki, M., and Jaffe, L.A. (1991). Organization of the sea urchin egg endoplasmic reticulum and its reorganization at fertilization. J. Cell Biol. *114*, 929–940.

Terasaki, M., Jaffe, L.A., Hunnicutt, G.R., and Hammer, III, J.A. (1996). Structural change of the endoplasmic reticulum during fertilization: evidence for loss of membrane continuity using the green fluorescent protein. Dev. Biol. *179*, 320–328.

Tilney, L.G., and Jaffe, L.A. (1980). Actin, microvilli and the fertilization cone of sea urchin eggs. J. Cell Biol. *87*, 771–782.